PHILOSOPHICAL TRANSACTIONS OF THE ROYAL SOCIETY A MATHEMATICAL, PHYSICAL & ENGINEERING SCIENCES

Dynamics of the Lithosphere and the Intraplate Stress Field [and Discussion]

M. J. R. Wortel, M. J. N. Remkes, R. Govers, S. A. P. L. Cloetingh, P. Th. Meijer and M. H. P. Bott

Phil. Trans. R. Soc. Lond. A 1991 **337**, 111-126
doi: 10.1098/rsta.1991.0110

Dynamics of the lithosphere and the intraplate stress field

By M. J. R. Wortel[1], M. J. N. Remkes[1], R. Govers[1], S. A. P. L. Cloetingh[2] and P. Th. Meijer[1]

[1] *Department of Geophysics, Institute of Earth Sciences, University of Utrecht, P.O. Box 80.021, 3508TA Utrecht, The Netherlands*

[2] *Department of Sedimentary Geology, Institute of Earth Sciences, Free University, De Boelelaan 1085, 1081HV Amsterdam, The Netherlands*

We outline the methodology of our numerical studies aimed at increasing the understanding of the relation between dynamics and stress field of the lithosphere with particular reference to oceanic lithosphere. The ridge-push force is modelled as a pressure gradient integrated over all contributing parts of the lithosphere. The slab-pull force is modelled as being dependent on the age of the subducting lithosphere. We parametrize the resistive forces and determine the unknown parameters by requiring the total torque of all forces acting on the plate to vanish. We illustrate the approach by the presentation and discussion of new modelling results for the Pacific plate.

1. Introduction

A variety of sources and processes is envisaged to contribute to the stress field in the lithosphere. Among these are dynamics of the lithosphere, heterogeneities in density structure and thickness of the crust and associated topography, bending processes and thermal stresses (see McNutt (1987) and Zoback *et al.* (1989) for recent reviews). In this paper we are concerned with the contribution arising from the dynamics of the lithosphere, that is the distribution of forces driving and resisting plate motion. Examples of studies in which the other contributions are addressed are Artyushkov (1973), Fleitout & Froidevaux (1982) and Froidevaux *et al.* (1988).

Studies of the dynamics of the lithosphere have followed two different approaches, both acknowledging that the dynamics of the Earth's lithosphere cannot be considered separately from the dynamics of the mantle: (*a*) one in which the plates are considered as principal units, and the interaction with the deeper mantle is parameterized in terms of forces or shear stresses acting along boundaries or the basal surface of the plates, and (*b*) the other in which emphasis is placed on the convecting mantle and the plates are considered to be the near-surface part of this system (Hager & O'Connell 1981; Forte & Peltier 1987; Vigny *et al.* 1991). Whereas the latter approach is appealing by virtue of its possible completeness and elegance, at present it does not allow as much detail of the stress field to be considered as does the former. Therefore, in this paper we focus on the former plate-wise approach for the dynamics of the lithosphere and use this approach as a basis for numerical calculations of the stress field in the lithosphere.

This approach requires a definition of the set of forces (referred to as 'plate-

Phil. Trans. R. Soc. Lond. A (1991) **337**, 111–126
Printed in Great Britain

tectonic forces') acting on lithospheric plates. Although pioneering studies of some of these forces, notably ridge push and slab pull, were made earlier (McKenzie 1969; Jacoby 1970), the study by Forsyth & Uyeda (1975) can be considered to mark the starting point of this plate force/torque approach (see also Chapple & Tullis 1977). They defined a set of forces acting on lithospheric plates, and assessed their relative importance. Also in search of the relevance of the various types of forces, Richardson *et al.* (1979) carried out an extensive series of numerical model calculations of the lithospheric stress field caused by plate-tectonic forces. The main difference between the studies by Richardson *et al.* (1979) and Forsyth & Uyeda (1975) and the approach outlined here (see also Wortel & Cloetingh 1981, 1983, 1985; Cloetingh & Wortel 1985, 1986) is that we consider some of the forces, in particular those driving the plates, to be well enough known to treat them as 'known' forces in the analysis. This is possible because the nature of the ridge push has been recognized to be that of an integrated pressure gradient (Lister 1975) and the dependence of this force and of slab pull (Vlaar & Wortel 1976) on lithospheric age has been established and because the age distribution of virtually all oceanic lithosphere is known (see Larson *et al.* 1985). By applying a balance of torques (of the forces acting on a plate), similar to that of Forsyth & Uyeda's (1975) study, quantitative information concerning the resistive forces can be obtained.

Because the forces acting on oceanic lithosphere are simpler (or better understood) than those acting on continental lithosphere, oceanic lithosphere provides a better opportunity to test whether plate-tectonic forces play a significant role in the stress field. Therefore, in this paper the emphasis will be on oceanic lithosphere. We outline basic aspects of our analysis of lithosphere dynamics and of the intraplate stress field and illustrate them by the presentation and discussion of new modelling results for the Pacific plate. Wherever this is appropriate, however, we draw on results obtained in earlier work.

2. Dynamics

(*a*) *General aspects*

The main aspects of the dynamic approach are illustrated in figure 1 (see also table 1), showing oceanic lithosphere with an accreting boundary (spreading ridge, on the right) and a subduction-zone boundary. With some rather straightforward modifications the analysis can be generalized to include continental lithosphere. In discussing the various forces we use the following definitions: (*a*) a force is specified per unit length of the boundary of the plate along which (or per unit area over which) it acts on the plate; the total force of each type acting on a particular plate is obtained by integration over the appropriate boundary or area, and (*b*) each force (say $\boldsymbol{F}_a$) is factorized into a product of a scalar quantity (F_a) representing the magnitude of the force per unit length of a boundary (for boundary forces) or per unit area (for surface forces) and a unit vector ($\hat{\boldsymbol{e}}_a$) giving the orientation of the force: $\boldsymbol{F}_a = F_a \hat{\boldsymbol{e}}_a$.

The forces which drive the plates are the ridge push $\boldsymbol{F}_{rp}$ and the slab pull $\boldsymbol{F}_{sp}$. The ridge-push force is not a boundary force acting at the ridge axis but a pressure gradient integrated over the area of the plate (Lister 1975). This pressure gradient results from the cooling and densification of the lithosphere. Therefore, contributions to the ridge push come from all parts of the oceanic lithosphere which are subject to continued cooling, that is all oceanic lithosphere younger than approximately 90 Ma (which is taken as the cut-off age).

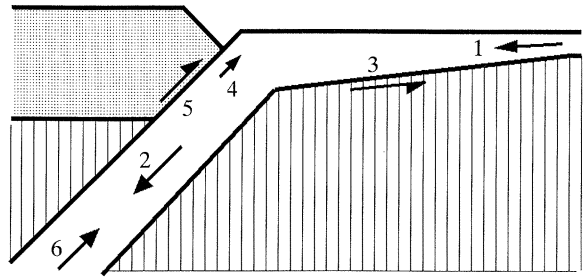

Figure 1. Schematic cross section of oceanic lithosphere, including ridge and trench, with an indication of forces used in the modelling: 1, ridge push F_{rp}; 2, slab pull F_{sp}; 3, drag force at the base of the lithosphere F_{dr} (alternatively called shear stress σ_b); 4, compositional buoyancy force F_{cb}; 5, resistance at plate contact F_{pc}; 6, deep resistance to slab penetration F_{sr}. Not shown are F_{up} (7), the force acting (at the plate contact) on the upper (overriding) plate, and F_{tf} (8), the resistive force acting along transform boundaries.

Table 1. *Force definition* (*see also figure 1*)

no.	force	symbol	no.	force	symbol
1	ridge push	F_{rp}	5	plate contact resistance	F_{pc}
2	slab pull	F_{sp}	6	deep resistance	F_{sr}
3	drag force	F_{dr}	7	upper plate resistance	F_{up}
4	compositional buoyancy	F_{cb}	8	transform fault resistance	F_{tf}

The ridge push, for a section (of unit width) of lithosphere from spreading ridge to age t, is calculated after Richter & McKenzie (1978),

$$F_{rp} = gh[\rho_m - \rho_w][\tfrac{1}{3}L + \tfrac{1}{2}h], \tag{1}$$

where g is the gravitational acceleration, h is the difference in elevation between the ridge crest and the ocean floor, L is the lithospheric thickness and ρ_w and ρ_m are the densities of seawater and of the sublithospheric mantle, respectively. Both L and h increase with age t according to a square-root-of-age relation, at least for $t < 70$ Ma (Crough 1975). This results in:

$$F_{rp} = c_{rp}\, t, \tag{2}$$

where c_{rp} is a constant. In our modelling the total ridge-push force is distributed over the area of the plate, on the basis of the age distribution and the implicit spreading history.

The other driving force, the slab pull F_{sp}, is the downdip component of the gravitational body force acting on the dense subducted slab (McKenzie 1969; Jacoby 1970). Per unit length in the direction of the trench this can be expressed as:

$$F_{sp} = g \sin\phi \int_0^L \int_0^{S_{sz}} \Delta\rho \, dx \, dz. \tag{3}$$

Here, ϕ is the dip and L the thickness of the downgoing slab, and $\Delta\rho$ the density contrast between slab and surrounding mantle. The x- and z-directions are downdip and perpendicular to the upper (dipping) interface between the slab and the upper mantle, respectively. The downdip integration is limited to the end of the seismic

zone (S_{sz}), which is reasonable in view of the drastic change in constitution (rheology) and subsequent deformation beyond this point (Wortel & Vlaar 1988). Using McKenzie's (1969) thermal model we find

$$F_{sp} = (4g\alpha\rho_m T_m L^3/\kappa\pi^4)\nu_c \sin\phi[1-\exp(-\pi^2\kappa S_{sz}/\nu_c L^2)], \quad (4)$$

where ν_c is the rate of plate convergence. The parameters α, ρ_m, T_m and κ are the coefficient of thermal expansion, the density and the temperature of the asthenosphere, and the thermal diffusivity of the asthenosphere/lithosphere respectively. For the present purpose, all these parameters may be taken to be constant. Using the age dependence of L (see above), $\kappa = 0.9\times10^{-6}$ m^2 s^{-1} and $S_{sz} = 0.12\,\nu_c t$ (see Wortel & Vlaar 1988) we obtain

$$[1-\exp(-\pi^2\kappa S_{sz}/\nu_c L^2)] = 0.29.$$

Thus the factor between brackets in (4) depends neither on ν_c nor on the age of the lithosphere. Putting $\nu_c \sin\phi = \nu_z$, it is found that

$$F_{sp} \propto \nu_z L^3. \quad (5a)$$

Taking into account the age-dependence of L gives

$$F_{sp} = c_{sp}\nu_z t^{\frac{3}{2}}, \quad (5b)$$

where c_{sp} is a constant. On the basis of their established age-dependence the driving forces $\boldsymbol{F}_{rp}$ and $\boldsymbol{F}_{sp}$ can be calculated. Information on the age distribution of oceanic lithosphere is taken from Larson *et al.* (1985).

The resistive forces shown in figure 1 (see also table 1) are the drag force $\boldsymbol{F}_{dr}$ acting at the base of the lithosphere (alternatively referred to as shear stress σ_b at the base of the plate) and three resistive forces acting on the downgoing slab in the trench region and in the upper-mantle part of the subduction zone. These three resistive forces, all of which are expressed as boundary forces per unit length in the direction of the strike of the subduction zone (trench axis), are: the compositional buoyancy force $\boldsymbol{F}_{cb}$ (acting in the up-dip direction of the subducting slab) and resistive shearing forces $\boldsymbol{F}_{pc}$ (representing the integrated value of the shear stress σ_{pc} along the plate contact with the overriding plate) and $\boldsymbol{F}_{sr}$ (the integrated value of σ_{sr}, the resistance to slab penetration in the upper mantle, taken to act upwards parallel to the dip of the slab). $\boldsymbol{F}_{cb}$ is associated with the petrological stratification of the oceanic crust and upper mantle created during the spreading process (Vlaar & Wortel 1976; Oxburgh & Parmentier 1977; England & Wortel 1980); both the basaltic crust and the depleted uppermost mantle are less dense than the adjacent upper mantle would be at an equivalent temperature and pressure. This density structure contributes a gravitationally stable component to the lithosphere/asthenosphere system. Upon subduction this is felt as a force ($\boldsymbol{F}_{cb}$) which counteracts the gravitationally unstable component resulting from the cooling and densification of the lithosphere which is represented by $\boldsymbol{F}_{sp}$. As noted by England & Wortel (1980) it is probable that the compositional buoyancy of the descending lithosphere is removed by phase changes at less than 100 km depth. Consequently, we estimate the magnitude of this force by integrating the (compositional) density difference of the dipping oceanic lithosphere down to a depth of 100 km (value given below). Not displayed in the cross section of figure 1, but included in the modelling, are the resistive force $\boldsymbol{F}_{tf}$ along transform faults, and the force $\boldsymbol{F}_{up}$ acting on the upper plate at the plate contact (counterpart of $\boldsymbol{F}_{pc}$ acting on subducting plate). In specific cases, different from the entirely

PHILOSOPHICAL TRANSACTIONS OF THE ROYAL SOCIETY A MATHEMATICAL, PHYSICAL & ENGINEERING SCIENCES

oceanic plate considered in figure 1, some other forces (not indicated in figure 1) may be relevant, like drag beneath the continents and the forces associated with continental collision (see Cloetingh & Wortel 1985, 1986).

To ensure mechanical equilibrium, the net torque (with respect to the Earth's centre) exerted by the forces on a plate is required to vanish:

$$\sum_N \int_P \boldsymbol{r} \times \boldsymbol{F} \, \mathrm{d}p = 0, \tag{6}$$

where the sum is over the total set of N forces and the integration is over the boundaries or the area of the plate P, depending on the nature of the force involved (boundary force or surface force). Of the forces considered above, the drag force at the base of the lithosphere ($\boldsymbol{F}_{\mathrm{dr}}$, or shear stress σ_{b}) and the ridge push ($\boldsymbol{F}_{\mathrm{rp}}$) are distributed over the area of the plate, whereas the other forces (see table 1, figure 1) are all modelled as boundary forces, either along the convergent (subduction zone) boundaries or (in case of $\boldsymbol{F}_{\mathrm{tf}}$) along transform fault boundaries. In the case of subduction-zone boundaries the trench axis is adopted as the geometrical boundary of the plate.

Solomon & Sleep (1974) applied a balance of torques to the combined set of all plates. In their study, which was directed at assessing the absolute motions of the plates, this was a useful formulation. As we shall proceed from dynamics and motion towards stress calculation we are interested in the entire set of forces acting on a plate, including forces distributed symmetrically along plate boundaries which do not contribute to a globally integrated torque but do contribute to the torque integrated for an individual plate.

(*b*) *Application and results*

We illustrate the procedure for the case of the Pacific plate. Figure 2 gives the age distribution (after Larson *et al.* 1985) used in the calculation of the slab pull and ridge push. Additional age data for the relatively young (Miocene–Oligocene) region southwest of the Marianas were incorporated after Weissel & Anderson (1978).

Several absolute motion models (Minster & Jordan 1978 (AM1-2); Chase 1978; Gripp & Gordon 1990 (HS2-NUVEL1)) have been used in the analysis. The difference between results obtained with different absolute motion models appeared to be insignificant. Values displayed or given below are those for the HS2-NUVEL1 model (Gripp & Gordon 1990).

Relative-motion models are generally derived from a data set comprising spreading rates at oceanic spreading centres, transform fault azimuths and slip vectors of earthquakes at the plate contact in subduction zones (see Demets *et al.* (1990) for a recent application and results). For the relative motion between the Pacific plate and neighbouring plates the various relative motion models are similar. For our modelling we used the relative motion data according to Scotese *et al.* (1988).

Whereas it is (relatively) clear, in particular with the nature of the ridge push as given above, where the driving forces act upon the lithosphere, it is considerably less evident where the various resistive forces (except $\boldsymbol{F}_{\mathrm{cb}}$ and $\boldsymbol{F}_{\mathrm{tf}}$) are exerted. Our analysis yields a significant trade-off for resistive-force magnitudes.

To reduce the number of unknowns we choose to adopt values for some resistive forces. On the basis of model results obtained by vanden Beukel (1990) we choose $F_{\mathrm{cb}} = 3.0 \times 10^{12}$ N m^{-1}, and for the force associated with transform faults we take

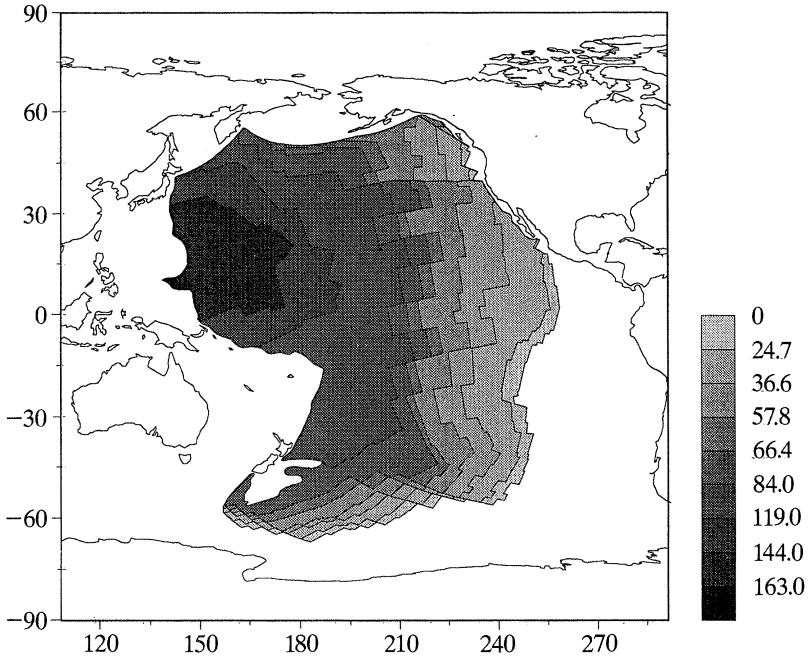

Figure 2. Age distribution of Pacific plate (after Larson *et al.* 1985). Values in legend are in millions of years.

$F_{tf} = 0.5 \times 10^{12}$ N m^{-1}. The latter value is in agreement with shear-stress values inferred for the San Andreas fault system (Zoback *et al.* 1987); we note, however, that the analysis appears to be quite insensitive to reasonable variations in the assumed value for F_{tf}. The remaining unknown resistive forces (or shear stresses) are $\boldsymbol{F}_{pc}$, $\boldsymbol{F}_{sr}$ and $\boldsymbol{F}_{dr}$ (or σ_b). The directions of these forces follow from the adopted relative and absolute motion models; and, theoretically, the three magnitudes F_{pc}, F_{sr} and σ_b (each of which is assumed uniform for the plate) can be determined by solving vector equation (6). The resulting solution, however, shows a negative value for the magnitude F_{pc} which corresponds to a driving force. For a plate contact force this is considered to be physically unrealistic. Therefore, negative values of F_{pc} are not accepted. By not accepting negative values of F_{pc}, however, we leave out the solution with a zero net torque. Hence, any other solution will show a net torque residue. The minimum value for the torque residue was found for $F_{sr} = 2.0 \times 10^{13}$ N m^{-1}. The corresponding trade-off relation between F_{pc} and the shear stress at the base of the lithosphere σ_b is shown in figure 3.

The torque residues have been normalized by the magnitude of the torque of the slab pull of the 'old' subduction zones (i.e. zones consuming lithosphere older than 90 Ma). For a given absolute motion model the trade-off relation between σ_b and F_{pc} is entirely a function of the geometry of the plate (surface area) and the distribution of subduction zones along its plate boundaries.

The torque residue appears to be rather insensitive to variations in σ_b for values less than *ca.* 0.3 MPa (3 bar). The minimum in the residues corresponds to a value for F_{pc} equal to zero. This is still physically unrealistic, and for the subsequent stress calculations we avoid such a non-positive value (i.e. a non-resistive plate contact

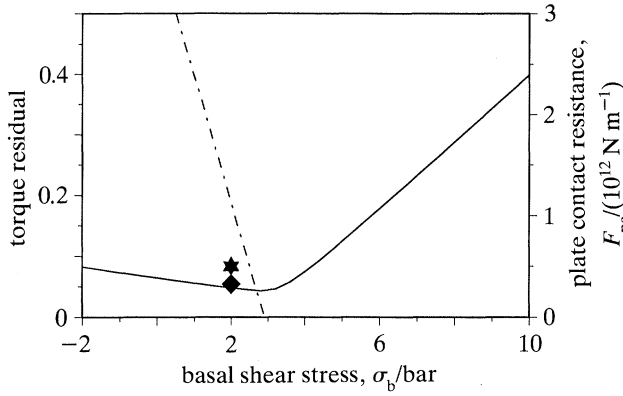

Figure 3. Trade-off in resistive forces. ————, Trade-off between shear stress at the base of the lithosphere σ_b and the resistance at the plate contact F_{pc} (vertical axis on the right). 10 bar = 1 MPa. ——, Residual of net integrated torque normalized by the magnitude of the torque of the slab pull of the 'old' slabs (vertical axis on the left). The asterisk indicates the values of the combination of σ_b and F_{pc} used in the stress calculation; the black square symbol indicates the corresponding residual torque. Deep resistance: $F_{sr} = 2 \times 10^{13}$ N m^{-1}.

Table 2. *Torque results*[a]

force		T_x	T_y	T_z	magnitude	lon. (°E)	lat. (°N)
ridge push	F_{rp}	1.836	2.011	−14.404	14.659	47.61	−79.29
slab pull (old)	F_{spo}	−3.015	57.462	−93.751	110.001	92.99	−58.45
slab pull (young)	F_{spy}	−0.096	12.756	−1.496	12.844	90.42	−6.69
drag force	F_{dr}	1.860	−5.961	10.594	12.297	−72.67	59.48
buoyancy	F_{cb}	0.599	−16.835	15.033	22.578	−87.95	41.74
plate contact (old)	F_{pco}	0.540	−0.677	2.152	2.320	−51.43	68.08
plate contact (young)	F_{pcy}	1.081	−0.757	1.511	2.006	−34.98	48.86
deep resistance	F_{sr}	2.441	−46.523	75.903	89.060	−86.99	58.45
upper plate	F_{up}	−0.466	0.106	0.874	0.996	167.33	61.34
transform fault	F_{tf}	0.664	−0.119	1.695	1.824	−10.17	68.28

[a] Torques are specified in units of 10^{25} N m, using a coordinate system with the origin in the Earth's centre and the x-axis through (0° N, 0° E), the y-axis through (0° N, 90° E) and the z-axis through the North Pole.

resistance) in our modelling. Therefore, we choose the combination of σ_b and F_{pc} indicated by the asterisk (see also §3).

The numerical values of the resulting torque vectors are given in table 2. Figure 4 gives a schematic display. The ridge-push torque is about an order of magnitude smaller than the slab-pull torque. This partially results from the age distribution in the northern and southern parts of the Pacific plate (E–W isochrons) which causes an internal compensation of the ridge-push torque.

Of particular interest is the question of compensation of the slab-pull forces by resistive forces acting in the subduction-zone area. As Solomon & Sleep (1974) and Chapple & Tullis (1977) realized, net subduction forces exerted on a plate from a long convergent plate-boundary may give rise to intraplate stresses of considerable magnitude. Indeed, our way of modelling the dynamics of the plate results in net forces acting along subduction zones. They are responsible for the tensional stresses in the northwestern part of the Pacific plate (§3, figure 5).

PHILOSOPHICAL TRANSACTIONS OF THE ROYAL SOCIETY A MATHEMATICAL, PHYSICAL & ENGINEERING SCIENCES

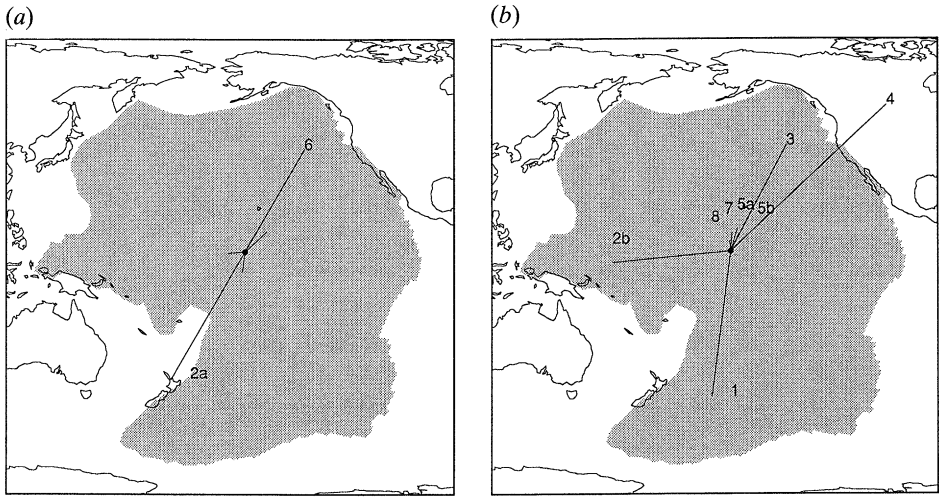

Figure 4. Schematic representation of torques: 2a and 2b indicate torque of slab pull for subduction zones for which the age of the descending lithosphere is older and younger than 90 Ma, respectively. A similar division (5*a* and 5*b*) is made for $\boldsymbol{F}_{\mathrm{pc}}$, the plate contact resistance. Other numbers correspond to those given in figure 1 (see also table 1). (*a*) All torques (not all are visible); (*b*) enlarged version of (*a*), but without torques of 'old' slab pull (2a) and deep resistance (6).

Adding the torques $\boldsymbol{T} = \int_{L_{\mathrm{conv}}} \boldsymbol{r} \times \boldsymbol{F}\,\mathrm{d}L$ of all forces acting in or along the convergent plate boundaries (L_{conv}) of the Pacific plate gives

$$|\boldsymbol{T}_{\mathrm{sp}} + \boldsymbol{T}_{\mathrm{up}} + \boldsymbol{T}_{\mathrm{pc}} + \boldsymbol{T}_{\mathrm{cb}} + \boldsymbol{T}_{\mathrm{sr}}|/|\boldsymbol{T}_{\mathrm{sp}}| = 0.05.$$

Thus upon torque integration over the convergent boundaries the compensation is nearly complete.

Finally, in spite of the insensitivity of the torque residue to variations in σ_{b}, our results do show some preference for positive values of σ_{b}, which in our analysis correspond to a resistive shear-stress at the base of the lithosphere.

3. Stress

(*a*) *General aspects*

For a rheological model of the lithosphere the stress field in the lithosphere associated with the plate-tectonic forces can be calculated numerically. This field, which is called the regional stress field, represents the non-lithostatic state of stress in the lithosphere. (It is often referred to as the deviatoric stress field, although the stress tensor is not necessarily deviatoric.) Because the stress values are to be compared with the strength distribution in the lithosphere, which is expressed in terms of differential stress, the lithostatic part of the stress field (depth-dependent pressure) can be omitted. Finite-element codes are used to carry out the calculations. The mesh for the plate consists of an assembly of triangular elements. The plates are modelled (with a plane stress approximation) as being elastic with a reference thickness of 100 km, Young's modulus $E = 7 \times 10^{10}$ N m^{-2} and Poisson's ratio $\nu = 0.25$. No physical significance should be attached to this chosen reference thickness. From model results for this rheology the stresses in a plate with a non-uniform thickness or a more complex rheology (see Goetze & Evans 1979) can be derived. As an example we mention the study by Stein *et al.* (1987) in which stresses calculated

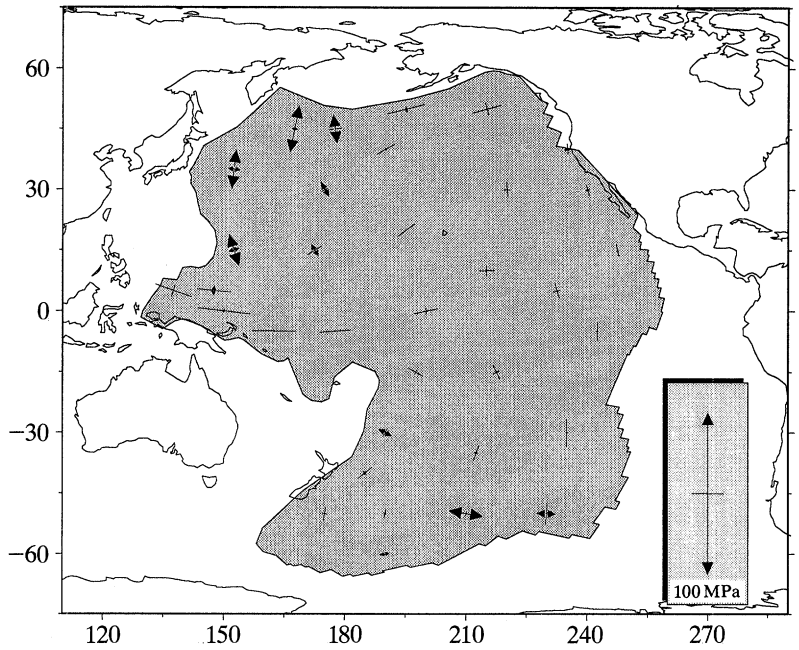

Figure 5. Calculated stress field of the Pacific plate. Plotted are the principal horizontal non-lithostatic stresses averaged over a uniform elastic plate with a reference thickness of 100 km. Principal axes with arrow-heads indicate tension, without arrow-heads compression. Scale is given in the lower-right corner.

for the Indo-Australian plate, on the basis of an assumed uniform plate thickness (100 km), were rescaled to stresses in the plate with an age-dependent thickness.

(*b*) *Stress field of the Pacific plate*

In principle it would be interesting to investigate the effect which varying the combination of F_{pc} and σ_b (according to figure 3) would have on the calculated stress field. Any non-zero torque, however, introduces reaction forces in the numerical procedure resulting in non-realistic features in the stress field. The magnitude of these forces increases with increasing magnitude of the torque residue. Combining the need for the torque residue to be as small as possible and the choice (see §2) that F_{pc} should be non-zero and positive led us to select the combination of values of F_{pc} and σ_b indicated by the asterisk in figure 3. The corresponding torque residue (square symbol in figure 3) is very near the minimum value.

The computational results for the intraplate stress field are shown in figure 5. The level of intraplate stress is moderate, typically in the order of 30 MPa (300 bar) or less (as displayed for a reference thickness of the plate).

4. Tests

(*a*) *Dynamics and plate motion*

We can test the force modelling by the procedure proposed by Gordon *et al.* (1978). They proposed that the absolute motion of a plate is governed by the integrated torque of the driving forces acting on the plate, slab pull and ridge push. In other words, the torque of the driving forces parallels the rotation vector describing

Figure 6

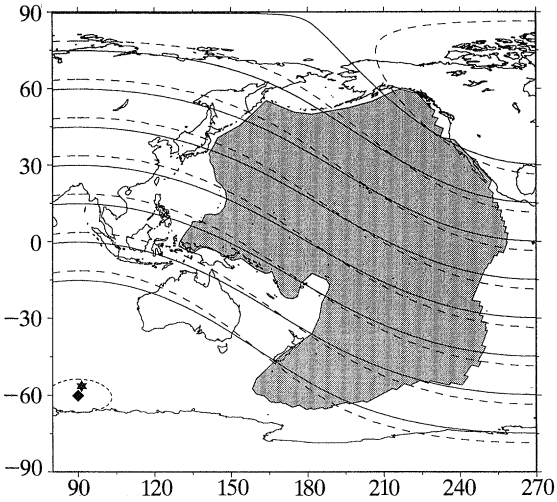

Figure 7

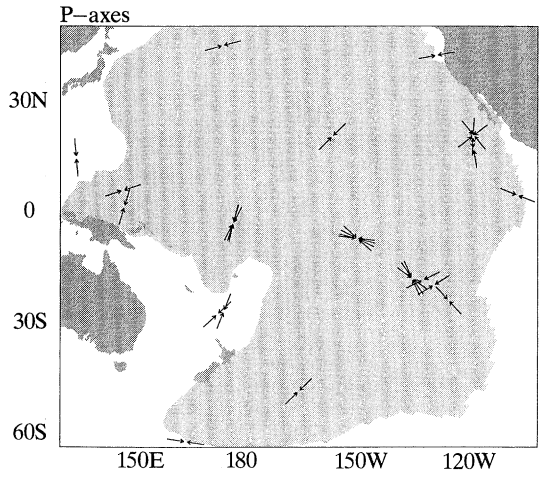

Figure 6. Relation between driving forces and absolute motion for the Pacific plate. Black square symbol: pole of absolute motion vector according to HS2-NUVEL1 (Gripp & Gordon 1990; see also DeMets *et al.* 1990). Solid curves are corresponding small circles. Asterisk: pole of integrated torque vector of driving forces (slab pull and ridge push). Dashed curves are corresponding small circles.

Figure 7. P-axes of focal mechanisms of intraplate earthquakes in the Pacific (World Stress Map database; Zoback *et al.* 1989).

absolute plate-motion. In their original approach Gordon *et al.* (1978) made the assumption that slab pull and ridge push are constant per unit width and act perpendicularly to the relevant segments of the trench and the ridge respectively. If now we quantify the slab pull and the ridge push as forces dependent on lithospheric age and consider the ridge push no longer as a line force but as a distributed force (see above) we can apply the same test to the Pacific plate. Figure 6 shows the pole of the torque of $\boldsymbol{F}_{\mathrm{sp}}$ and $\boldsymbol{F}_{\mathrm{rp}}$ integrated over the plate. The predicted rotation pole falls within the error ellipse for the absolute motion model HS2-NUVEL1 (Gripp & Gordon 1990) which is based on Minster & Jordan's (1978) hot spot data and the NUVEL1 relative motion model (DeMets *et al.* 1990). This is in excellent agreement with the proposition of Gordon *et al.* (1978).

(*b*) *Stress field: orientation and magnitude*

(i) *Orientation*

The orientations of the principal stress axes as shown in figure 5 can be compared with observational data. The World Stress Map project was aimed at providing a data base for this purpose. For the Pacific plate, however, the available data-set is very limited in both quantity and quality (see Zoback *et al.* 1989). Nevertheless reasonable agreement between the calculated field (figure 5) and the focal mechanism data (figure 7), notably the rotation of stress axes in the central part of the Pacific plate and E–W oriented compression in the northwestern part, can be observed. The low level of seismic activity seems to be in qualitative agreement with the low level of stress inferred from our modelling.

For oceanic intraplate stress fields the best opportunity to employ stress information from seismicity to test our stress modelling is provided by the Indo-Australian plate. There are two reasons: (1) the level of seismic activity is high by

PHILOSOPHICAL TRANSACTIONS OF THE ROYAL SOCIETY A MATHEMATICAL, PHYSICAL & ENGINEERING SCIENCES

Figure 8

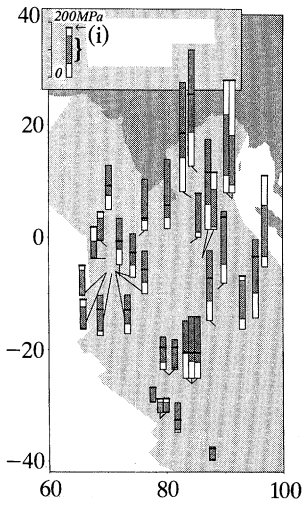

Figure 9

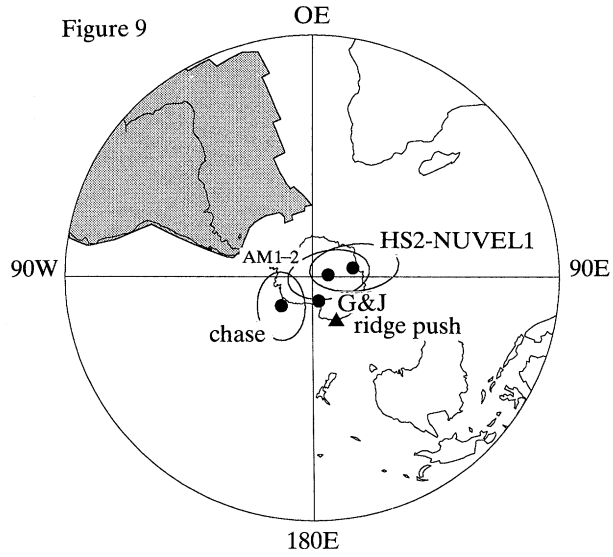

Figure 8. Stress magnitudes in the central Indian Ocean part of the Indo-Australian plate (grey shading). Plotted are the differential stresses at epicentral locations (see Govers *et al.* 1991) inferred from the hypocentral depths (see text). The ends of the thin solid lines at the base of the columns (if not present, the middle points of the base of the columns) indicate the epicentral locations. All stress values are expressed for a uniform reference value (100 km) of the plate thickness. The dark band in the column corresponds to the uncertainty in the inferred differential stress. The thicker horizontal line in the column gives the differential stress calculated by Cloetingh & Wortel (1985, 1986). (i) Stress from modelling ($\sigma_1 - \sigma_3$) from earthquakes.

Figure 9. Relation between driving forces and absolute motion for the South American plate. Circles: Poles of absolute-motion vectors for the South American plate, according to models AM1-2 (Minster & Jordan 1978), Gordon & Jurdy (1986, labelled G&J), Chase (1978), HS2-NUVEL1 (Gripp & Gordon 1990; see also DeMets *et al.* 1990). Triangle: pole of integrated torque vector of driving force (ridge push).

oceanic intraplate standards, and detailed studies of focal mechanisms are available (Wiens & Stein 1983, 1984; Bergman & Solomon 1984, 1985), and (2) for this plate Cloetingh & Wortel (1985, 1986) have calculated the stress field using the same procedure as outlined here.

For the Indo-Australian plate the agreement between calculated stress orientations and focal mechanism data is excellent (see Cloetingh & Wortel 1986; Bergman 1986). Also the orientations of observed long-wavelength basement undulations in the northeastern Indian Ocean appear to be consistent with calculated stress orientations (Stein *et al.* 1989).

(ii) *Magnitude*

Direct measurements of magnitudes of lithospheric stress are difficult to obtain. In a recent study we proposed a method to infer magnitude information from the depth of earthquake hypocentres. Using a lithospheric rheology model we relate the hypocentral depths of earthquakes quantitatively to the stress level in the lithosphere (see Govers *et al.* 1991). The depth-dependent rheology encompasses Byerlee's (1978) law, with the assumption of hydrostatic pore pressure, and flow laws derived for wet olivine (Tsenn & Carter 1987). Through the temperature-dependence of the flow laws, the dependence of the lithosphere's rheology on age is implicitly taken into account.

PHILOSOPHICAL TRANSACTIONS OF THE ROYAL SOCIETY A MATHEMATICAL, PHYSICAL & ENGINEERING SCIENCES

Since the strength value is taken to be the upper limit of the differential stress which can be supported elastically, Govers *et al.* (1991) adopted as a starting point of the analysis the fact that earthquakes do not occur at a certain depth if locally the stress is below the strength value. Hence, seismic activity indicates that the strength is reached. This enabled them to derive a minimum value for the differential stress $(\sigma_1 - \sigma_3)$ from the depth of an earthquake's hypocentre in combination with the depth-dependent strength distribution. Uncertainties in focal depth, in age of the lithosphere and in strain rate (both of which affect the temperature-dependent ductile portion of the strength envelope), and in the slope of the brittle part of the strength envelope result in an uncertainty in the inferred value for the differential stress. The method was applied using the earthquakes of the Central Indian Ocean lithosphere for which accurate depth determinations are available (Wiens & Stein 1983, 1984; Bergman & Solomon 1984, 1985). Figure 8 shows the range of differential stress inferred from the seismicity data and also the differential stress calculated by Cloetingh & Wortel (1986).

With the exception of some events in the northeastern part of the Central Indian Ocean the agreement between seismicity derived values and model calculations is good. Stress levels about an order of magnitude lower, as advocated by Richardson (1989), are not sufficient to explain the observed seismicity, at least not according to the model (and the rheologies) used. We note, however, that relating earthquake occurrence to lithospheric stress requires a model or hypothesis for the relation between the two, which at present is not well established.

5. Discussion

(*a*) *Orientation of* $S_{\mathrm{H,max}}$ *and direction of absolute motion*

Zoback *et al.* (1989) draw attention to the observation that for some plates there is a tendency for the orientation of $S_{\mathrm{H,max}}$ (maximum compressive stress) to be (sub)parallel to the direction of absolute motion, and subsequently discussed possible mechanisms which may account for this feature. From our analysis we arrive at the following preferred interpretation of this observation (and implicitly also of deviations from this pattern). The driving forces govern the direction of absolute motion (see figure 6). The resistive forces passively adjust themselves to this imposed direction. The stress field, on the other hand, is a function of the entire set of forces acting on the plate. Depending on the geometry of the plate and the distribution of plate boundaries involving subduction zones and spreading ridges the principal-stress axes may align with the direction of the small circles of the driving forces. Thus, such an alignment is not a fundamental feature of the stress field. For the Pacific plate, for example, this alignment tendency is weak and it breaks down for the western part of the plate roughly coinciding with the lithosphere older than 80 Ma. We attribute this to the configuration of the convergent plate boundaries in the northwestern part of the Pacific plate which are located not only along its western boundaries but also along the northern edge of the plate.

(*b*) *Level of stress*

Upon comparison of figures 5 and 8 we note that the model results for the Indo-Australian plate gave a considerably higher level of intraplate stress than our results for the Pacific plate. Above we have presented evidence in support of the high level of stress in the Indo-Australian plate. We note that the Pacific plate results are of the

PHILOSOPHICAL TRANSACTIONS OF THE ROYAL SOCIETY A MATHEMATICAL, PHYSICAL & ENGINEERING SCIENCES

same level of magnitude as earlier calculations of the stress level in the Nazca plate (Wortel & Cloetingh 1985; see also Richardson & Cox 1984). The difference in stress level between the Pacific plate, on the one hand, and the Indo-Australian plate on the other can be accounted for by the very different dynamic configuration of the plates involved. The Indo-Australian plate is characterized by high, and strongly non-uniformly distributed, resistance associated with continental collision, both in the Himalayan region and in the Banda arc. The Pacific plate does not encounter such high resistance, and the resistance is distributed more evenly. Hence, the slab pull forces can be compensated in a much smoother way thereby leading presumably to a situation with an approximate terminal velocity for subducting slabs, as invoked by Forsyth & Uyeda (1975). The same holds for the Nazca plate.

(*c*) *Other plates*

Through the choice of the Pacific plate the emphasis has been on oceanic lithosphere. The dynamics of this plate are strongly dominated by the slab-pull forces associated with the very long convergent plate boundaries. This renders the system insensitive to the magnitude of the smaller forces. The South American plate provides an interesting complementary situation. The ridge push is likely to be the main driving force, whereas the slab pull plays a very minor role (Lesser Antilles and South Sandwich subduction zones). Meijer & Wortel (1991) studied the dynamics of this plate in terms of a first-order model incorporating a ridge-push force $\boldsymbol{F}_{\mathrm{rp}}$, a drag force at the base of the lithosphere $\boldsymbol{F}_{\mathrm{dr}}$ (σ_{b}), a transform fault resistance $\boldsymbol{F}_{\mathrm{tf}}$, an upper plate resistance $\boldsymbol{F}_{\mathrm{up}}$ at the interface between the descending Nazca plate and the South American plate, and a resistive force associated with the contact between the South American plate and the Caribbean plate (called $\boldsymbol{F}_{\mathrm{Car}}$). For several segments of the plate's boundaries complications arise, the associated forces of which are largely unknown. They are dealt with in terms of superpositions onto the first-order model. Parameters specifying these additional forces (magnitude, azimuth) are determined from the torque balance constraint. Meijer & Wortel (1991) show that a large set of force distributions satisfies this constraint. This illustrates the need to consider specific aspects of an individual plate. By modelling the stress field (work in progress) it should be possible to discriminate between this large number of force distributions by using the observed stress directions.

A test similar to the one for the Pacific plate in figure 6, using Gordon *et al.*'s (1978) hypothesis, has been made for the South American plate. The magnitude of the ridge-push torque is 11.1×10^{25} N m, comparable with that of the Pacific plate (see table 2). In the absence of a significant slab-pull torque, however, the magnitude of the total torque of the driving forces is an order of magnitude smaller for the South American plate than for the Pacific plate. Nevertheless, the agreement between poles of absolute motion and the pole of the torque of the driving forces is good (see figure 9).

6. Conclusions

From our analysis of the Pacific plate we draw the following conclusions which we consider to be of general interest in the context of modelling dynamics and stress fields of the lithosphere.

1. Modelling the dynamics of the lithosphere via plate-tectonic forces satisfactorily

PHILOSOPHICAL TRANSACTIONS OF THE ROYAL SOCIETY A MATHEMATICAL, PHYSICAL & ENGINEERING SCIENCES

accounts for the direction of absolute motion, and provides a good basis for quantifying the contribution of tectonic forces to the intraplate stress field.

2. The slab pull acting on the subducted lithosphere is not necessarily compensated locally. When integrated over the full length of convergent plate boundaries, however, it is very nearly compensated by resistive forces. This lack of local compensation strongly affects the stress distribution in the plate.

3. Our numerical results show a preference for shear stresses at the base of the oceanic lithosphere to be resisting, rather than driving, plate motion.

4. A positive correlation between the orientation of $S_{\mathrm{H,\,max}}$ and the direction of absolute motion, which has been observed for some plates, is not a fundamental feature of the intraplate stress field. The entire set of forces acting on a plate should be considered. Depending on the nature and distribution of these forces an alignment of the two directions may or may not occur.

References

Artyushkov, E. V. 1973 The stresses in the lithosphere caused by crustal thickness inhomogeneities. *J. geophys. Res.* **78**, 7675–7708.

Bergman, E. A. 1986 Intraplate earthquakes and the state of stress in oceanic lithosphere. *Tectonophys.* **132**, 1–35.

Bergman, E. A. & Solomon, S. C. 1984 Source mechanisms of earthquakes near mid-ocean ridges from body waveform inversion: implications for early evolution of oceanic lithosphere. *J. geophy. Res.* **89**, 11415–11441.

Bergman, E. A. & Solomon, S. C. 1985 Earthquake source mechanisms from body-waveform inversion and intraplate tectonics in the northern Indian Ocean. *Phys. Earth planet. Int.* **40**, 1–23.

Byerlee, J. D. 1978 Friction of rocks. *Pageoph.* **116**, 615–626.

Chapple, W. M. & Tullis, T. E. 1977 Evaluation of the forces that drive the plates. *J. geophys. Res.* **82**, 1967–1984.

Chase, C. G. 1978 Plate kinematics: the Americas, East Africa, and the rest of the world. *Earth planet. Sci. Lett.* **37**, 355–368.

Cloetingh, S. & Wortel, R. 1985 Regional stress field of the Indian plate. *Geophys. Res. Lett.* **12**, 77–80.

Cloetingh, S. & Wortel, R. 1986 Stress in the Indo-Australian plate. *Tectonophys.* **132**, 49–67.

Crough, S. T. 1975 Thermal model of oceanic lithosphere. *Nature, Lond.* **256**, 388–390.

DeMets, C., Gordon, R. G., Argus, D. F. & Stein, S. 1990 Current plate motions. *Geophys. J. Int.* **101**, 425–478.

England, P. & Wortel, R. 1980 Some consequences of the subduction of young slabs. *Earth planet. Sci. Lett.* **47**, 403–415.

Fleitout, L. & Froidevaux, C. 1982 Tectonics and topography for a lithosphere containing density heterogeneities. *Tectonics* **1**, 21–56.

Forsyth, D. & Uyeda, S. 1975 On the relative importance of the driving forces of plate motion. *Geophys. Jl R. astr. Soc.* **43**, 163–200.

Forte, A. M. & Peltier, W. R. 1987 Plate tectonics and aspherical Earth structure. *J. geophys. Res.* **92**, 3645–3679.

Froidevaux, C., Uyeda, S. & Uyeshima, M. 1988 Island arc tectonics. *Tectonophys.* **148**, 1–9.

Goetze, C. & Evans, B. 1979 Stress and temperature in the bending lithosphere as constrained by experimental rock mechanics. *Geophys. Jl R. astr. Soc.* **59**, 463–478.

Gordon, R. G., Cox, A. C. & Harter, C. E. 1978 Absolute motion of an individual plate estimated from its ridge and trench boundaries. *Nature, Lond.* **274**, 752–755.

Gordon, R. G. & Jurdy, D. M. 1986 Cenozoic global plate motions. *J. geophys. Res.* **91**, 12389–12406.

Govers, R., Wortel, M. J. R., Cloetingh, S. A. P. L. & Stein, C. A. 1991 Stress magnitude estimates from earthquakes in oceanic plate interiors. *J. geophys. Res.* (In the press.)

PHILOSOPHICAL TRANSACTIONS OF THE ROYAL SOCIETY A MATHEMATICAL, PHYSICAL & ENGINEERING SCIENCES

Gripp, A. E. & Gordon, R. G. 1990 Current plate velocities relative to the hotspots incorporating the NUVEL-1 global plate motion model. *Geophys. Res. Lett.* **17**, 1109–1112.

Hager, B. H. & O'Connell, R. J. 1981 A simple model of plate dynamics and mantle convection. *J. geophys. Res.* **86**, 4843–4867.

Jacoby, W. R. 1970 Instability in the upper mantle and global plate movements. *J. geophys. Res.* **75**, 5671–5680.

Larson, R. L., Pitman III, W. C., Golovchenko, X., Cande, S. C., Dewey, J. F., Haxby, W. F. & LaBreque, J. C. 1985 The bedrock geology of the World. San Francisco: W. H. Freeman.

Lister, C. R. B. 1975 Gravitational drive on oceanic plates caused by thermal contraction. *Nature, Lond.* **257**, 663–665.

McKenzie, D. P. 1969 Speculations on the consequences and causes of plate motion. *Geophys. Jl R. astr. Soc.* **18**, 1–32.

McNutt, M. 1987 Lithospheric stress and deformation. *Rev. Geophys.* **25**, 1245–1253.

Meijer, P. Th. & Wortel, M. J. R. 1991 The dynamics of motion of the South American plate. *J. geophys. Res.* (In the press.)

Minster, J. B. & Jordan, T. H. 1978 Present-day plate motions. *J. geophys. Res.* **83**, 5331–5354.

Oxburgh, R. & E. M. Parmentier 1977 Compositional and density stratification in oceanic lithosphere. *J. geol. Soc. Lond.* **133**, 343–355.

Richardson, R. M., Solomon, S. C. & Sleep, N. H. 1979 Tectonic stress in the plates. *Rev. Geophys. Space Phys.* **17**, 981–1019.

Richardson, R. M. & Cox, B. L. 1984 Evolution of oceanic lithosphere: a driving force study of the Nazca plate. *J. geophys. Res.* **89**, 10043–10052.

Richardson, R. M. 1989 The origin of the intraplate stress field. *28th Int. Geol. Congress, Washington, Abstr. Vol.* **2**, 695–696.

Richter, F. M. & McKenzie, D. P. 1978 Simple plate models of mantle convection. *J. Geophys.* **44**, 441–471.

Scotese, C. R., Gahagan, L. M. & Larson, R. L. 1988 Plate tectonic reconstructions of the Cretaceous and Cenozoic ocean basins. *Tectonophys.* **155**, 27–48.

Solomon, S. C. & Sleep, N. H. 1974 Some simple physical models for absolute plate motions. *J. geophys. Res.* **79**, 2557–2567.

Stein, C. A., Cloetingh, S. & Wortel, R. 1989 SEASAT-derived gravity constraints on stress and deformation in the northeastern Indian Ocean. *Geophys. Res. Lett.* **16**, 823–826.

Stein, S., Cloetingh, S., Wiens, D. A. & Wortel, R. 1987 Why does near ridge extensional seismicity occur primarily in the Indian Ocean? *Earth planet. Sci. Lett.* **82**, 107–113.

Tsenn, M. C. & Carter, N. L. 1987 Upper limits of power law creep of rocks. *Tectonophys.* **136**, 1–26.

vanden Beukel, J. 1990 Thermal and mechanical modelling of convergent plate boundaries (Ph.D. thesis, University of Utrecht). *Geologica Ultraiectina* **62**. (126 pages.)

Vigny, C., Ricard, Y. & Froidevaux, C. 1991 The driving mechanism of plate tectonics. *Tectonophys.* **187**, 345–360.

Vlaar, N. J. & Wortel, M. J. R. 1976 Lithospheric aging, instability and subduction. *Tectonophys.* **32**, 331–351.

Weissel, J. K. & Anderson, R. N. 1978 Is there a Caroline plate? *Earth planet. Sci. Lett.* **41**, 143–158.

Wiens, D. A. & Stein, S. 1983 Age-dependence of oceanic intraplate seismicity and the implications for lithospheric evolution. *J. geophys. Res.* **88**, 6455–6468.

Wiens, D. A. & Stein, S. 1984 Intraplate seismicity and stress in young lithosphere. *J. geophys. Res.* **89**, 11442–11464.

Wortel, R. & Cloetingh, S. 1981 On the origin of the Cocos-Nazca spreading center. *Geology* **9**, 425–430.

Wortel, R. & Cloetingh, S. 1983 A mechanism for the fragmentation of oceanic plates. *AAPG Mem.* **34**, 793–801.

Wortel, M. J. R. & Cloetingh, S. A. P. L. 1985 Accretion and lateral variations in tectonic structure along the Peru-Chile Trench. *Tectonophys.* **112**, 443–462.

PHILOSOPHICAL TRANSACTIONS OF THE ROYAL SOCIETY A MATHEMATICAL, PHYSICAL & ENGINEERING SCIENCES

Wortel, M. J. R. & Vlaar, N. J. 1988 Subduction zone seismicity and the thermo-mechanical evolution of downgoing lithosphere. *Pageoph.* **128**, 625–659.

Zoback, M. D., *et al.* 1987 New evidence on the state of stress of the San Andreas fault system. *Science, Wash.* **238**, 1105–1111.

Zoback, M. L., *et al.* 1989 Global patterns of tectonic stress. *Nature, Lond.* **341**, 291–298.

Discussion

J. Cartwright (*Imperial College, London, U.K.*). Why do there appear to be no examples of compressional reactivation of extensional faults on a passive margin by the ridge-push force? Is this because the magnitude of the ridge-push force is too small even on old divergent margins?

M. J. R. Wortel. On the basis of the level of stress associated with the ridge-push force combined with the knowledge now available on the strength of the lithosphere (including lithosphere with pre-existing faults) we indeed consider this to be the principal cause. In the context of fault reactivation and seismic activity along passive margins we expect, however, that sources other than the ridge-push force, such as deglaciation and sediment loading, have to be envisaged as well.

M. H. P. Bott (*Durham University, U.K.*). The chief problem seems to be in assessing the slab-pull force. Does Dr Wortel's formula take into account the length of the slab?

M. J. R. Wortel. In calculating the slab-pull force the length of the slab was taken into account according to equation (3) which results from integrating the density difference (between the slab and the surrounding mantle) from the trench downdip to a distance S_{sz}. This parameter S_{sz} represents the downdip length of the Wadati–Benioff seismic zone associated with subducted oceanic lithosphere. A relation was derived from a global survey of subduction zones, and used in this paper, that S_{sz} varies with age t of the downgoing lithosphere according to $S_{sz} = 0.12\, v_c\, t$, where v_c is the convergence rate (with proper allowance for oblique convergence); see Wortel & Vlaar (1988) for a review. The above procedure implies that the slab-pull force in our modelling incorporates the anomalous density in the cold descending slab down to the depth of the deepest earthquake hypocentres in the subduction zone.

PHILOSOPHICAL TRANSACTIONS OF THE ROYAL SOCIETY A MATHEMATICAL, PHYSICAL & ENGINEERING SCIENCES

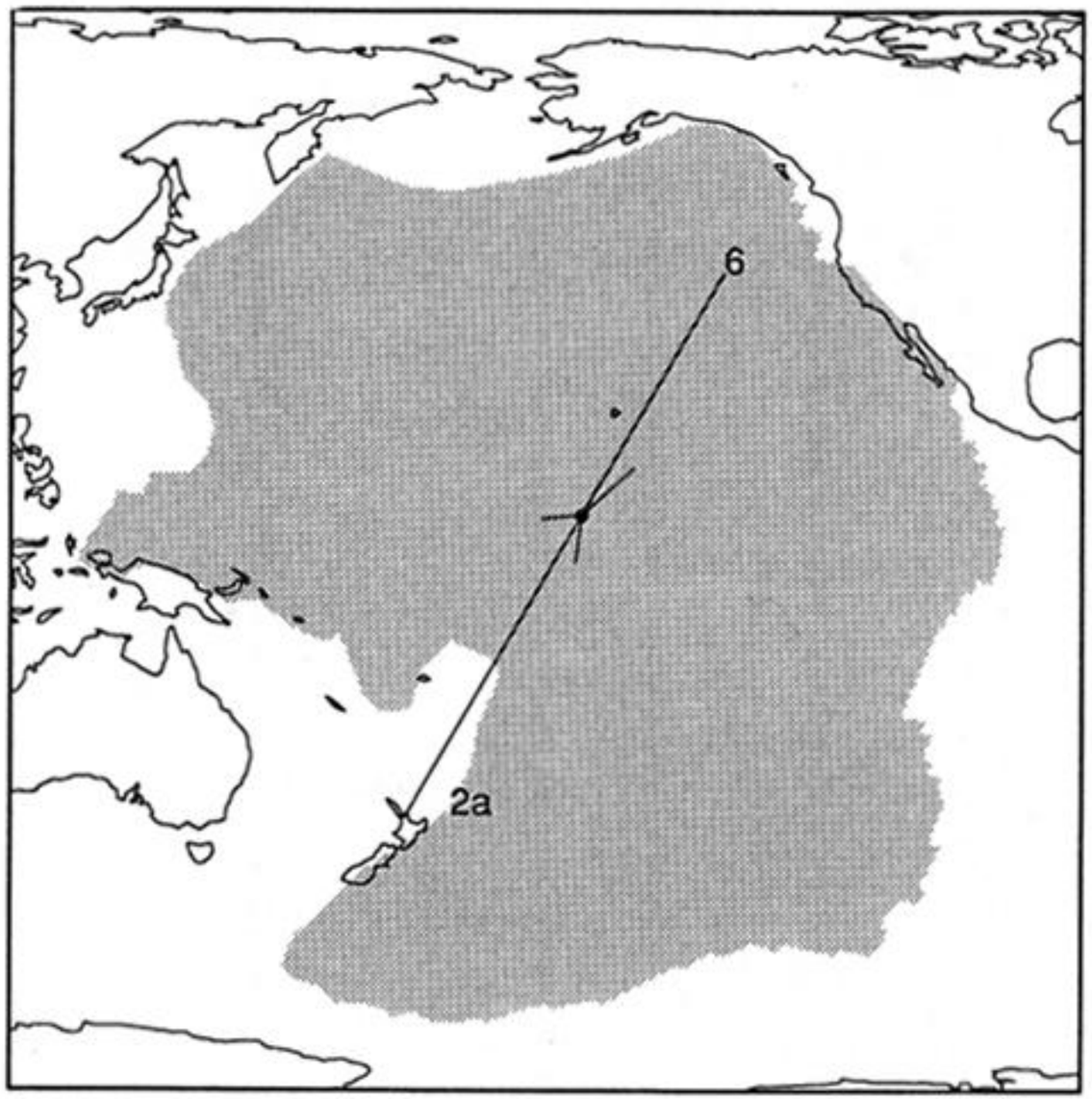

igure 4. Schematic representation of torques: 2a and 2b indicate torque of slab pull for subduction nes for which the age of the descending lithosphere is older and younger than 90 Ma, respectively. similar division ($5a$ and $5b$) is made for $\boldsymbol{F}_{\mathrm{pc}}$, the plate contact resistance. Other numbers rrespond to those given in figure 1 (see also table 1). (a) All torques (not all are visible); (b) larged version of (a), but without torques of 'old' slab pull (2a) and deep resistance (6).

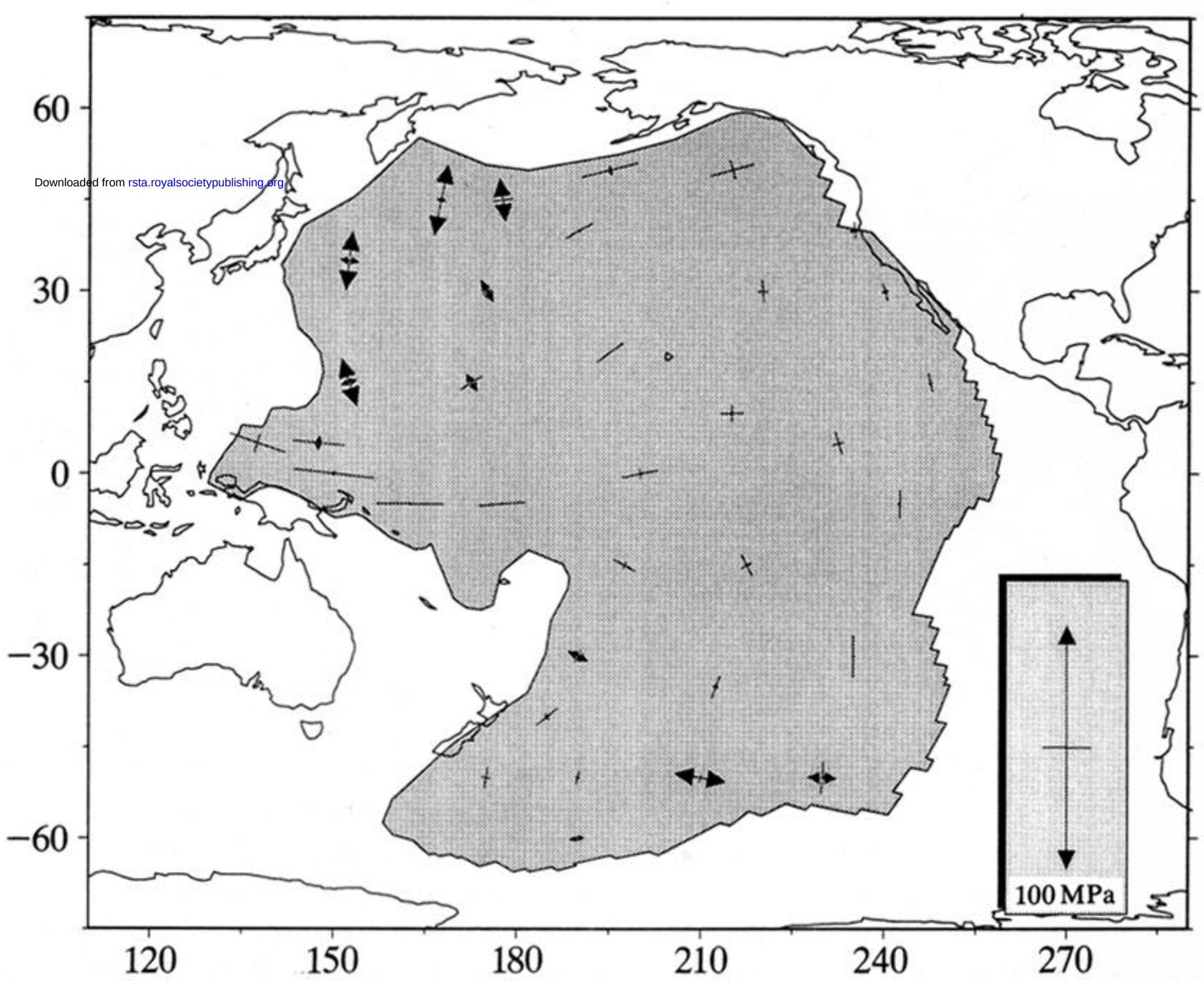

igure 5. Calculated stress field of the Pacific plate. Plotted are the principal horizontal non-
hostatic stresses averaged over a uniform elastic plate with a reference thickness of 100 km.
rincipal axes with arrow-heads indicate tension, without arrow-heads compression. Scale is given
the lower-right corner.

Figure 6

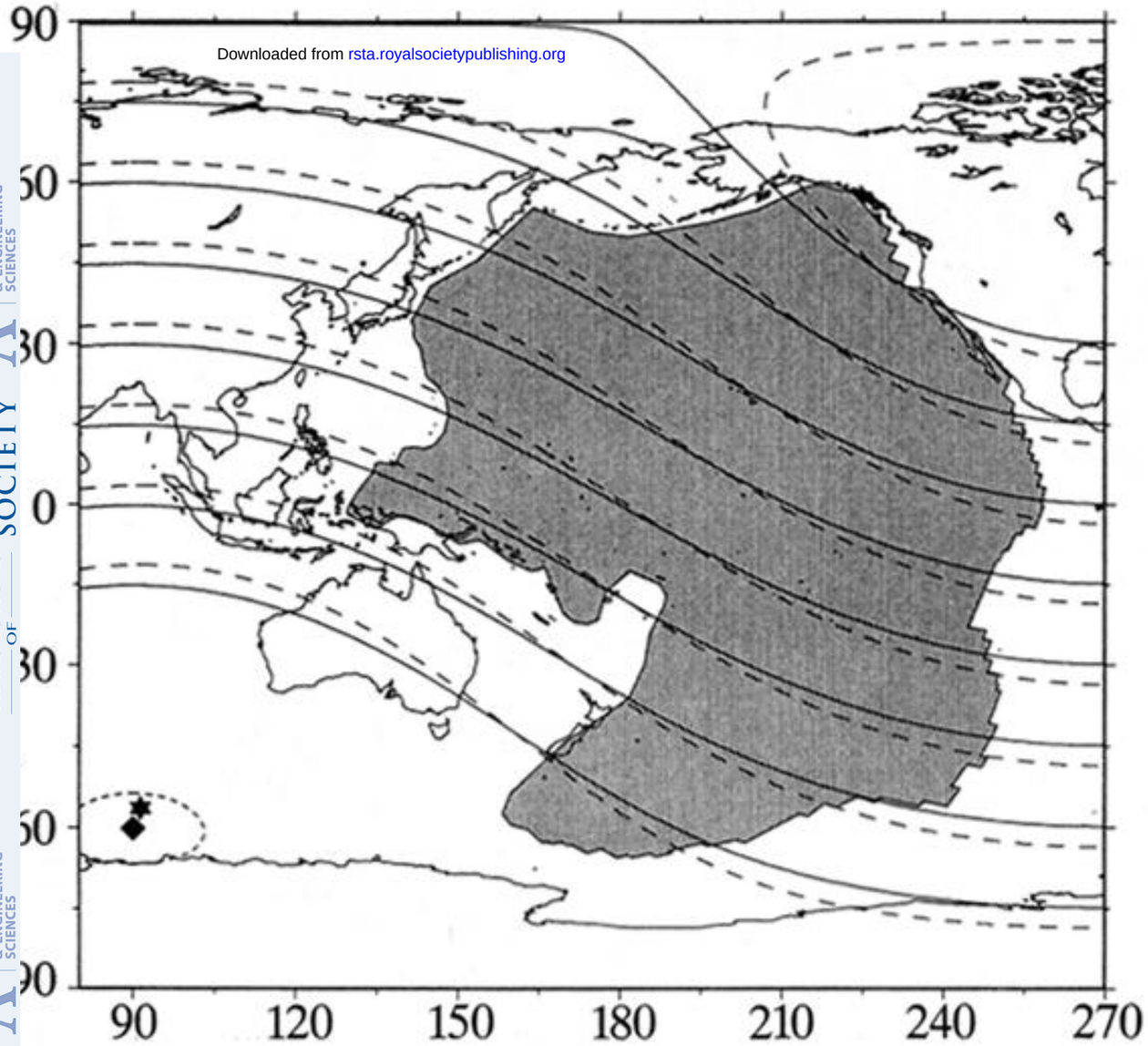

Figure 7

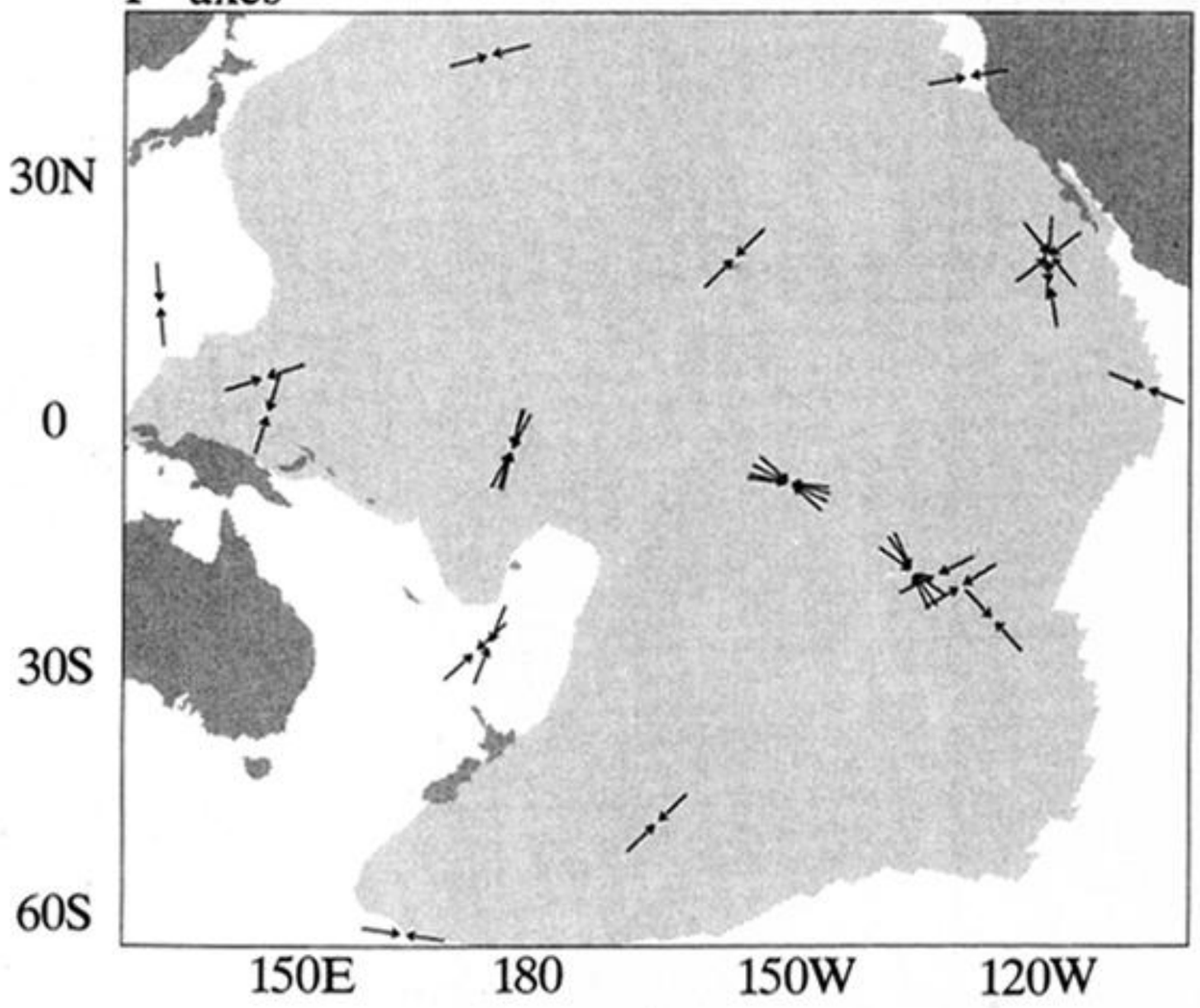

Figure 6. Relation between driving forces and absolute motion for the Pacific plate. Black square symbol: pole of absolute motion vector according to HS2-NUVEL1 (Gripp & Gordon 1990; see also DeMets *et al.* 1990). Solid curves are corresponding small circles. Asterisk: pole of integrated torque vector of driving forces (slab pull and ridge push). Dashed curves are corresponding small circles.

Figure 7. P-axes of focal mechanisms of intraplate earthquakes in the Pacific (World Stress Map database; Zoback *et al.* 1989).

Figure 8

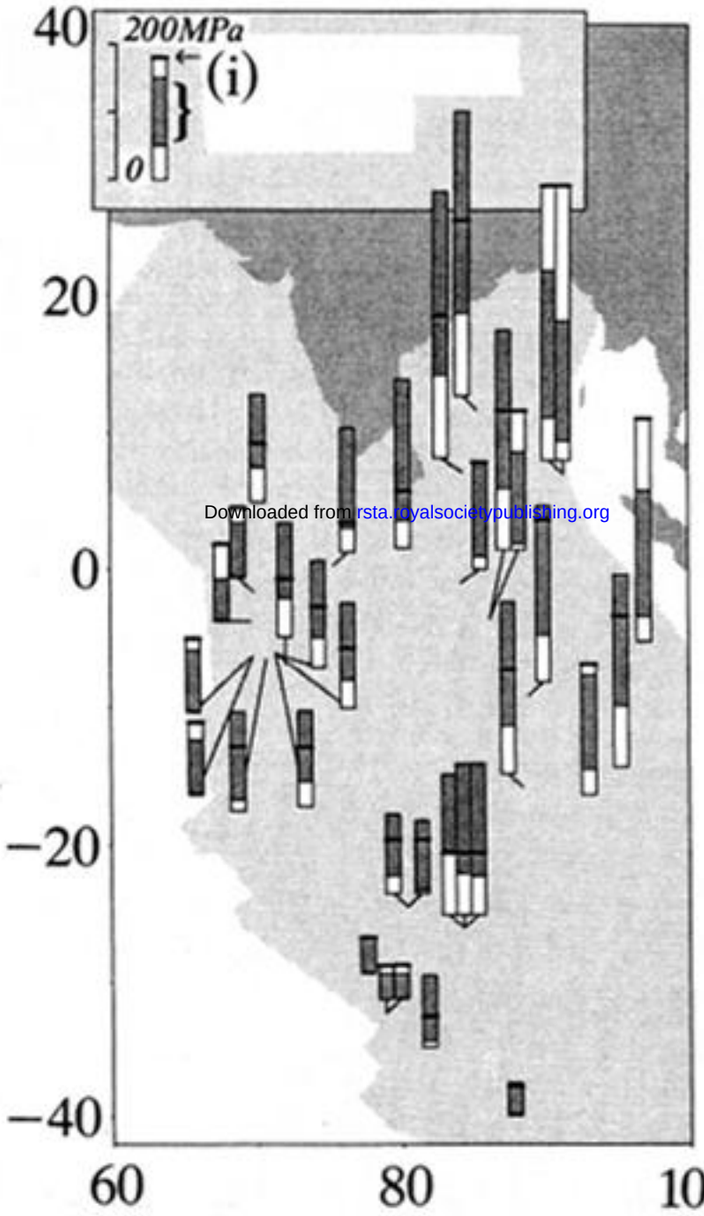

Figure 9

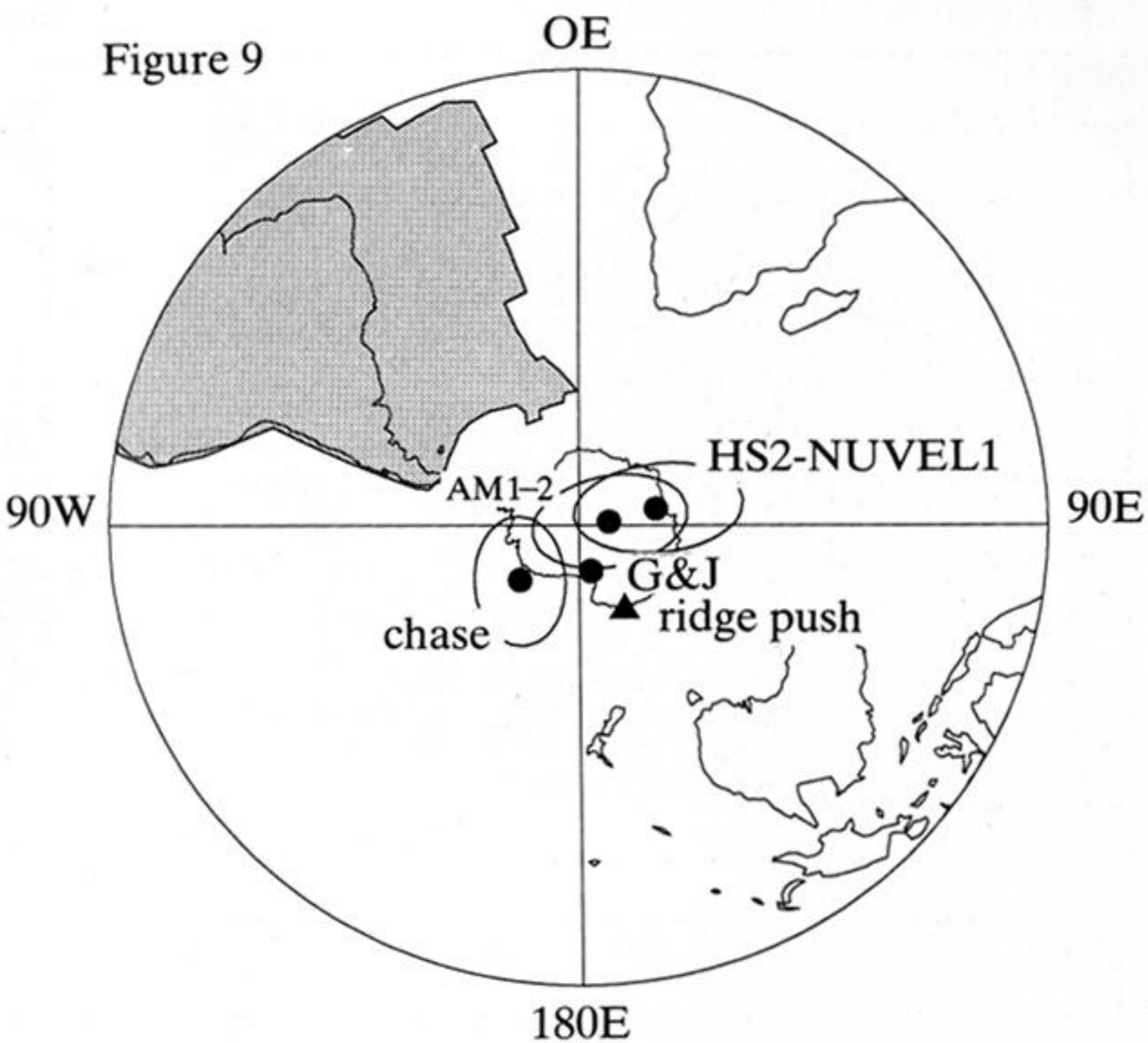

igure 8. Stress magnitudes in the central Indian Ocean part of the Indo-Australian plate (grey nading). Plotted are the differential stresses at epicentral locations (see Govers *et al.* 1991) inferred om the hypocentral depths (see text). The ends of the thin solid lines at the base of the columns f not present, the middle points of the base of the columns) indicate the epicentral locations. All ress values are expressed for a uniform reference value (100 km) of the plate thickness. The dark and in the column corresponds to the uncertainty in the inferred differential stress. The thicker orizontal line in the column gives the differential stress calculated by Cloetingh & Wortel (1985, 986). (i) Stress from modelling $(\sigma_1 - \sigma_3)$ from earthquakes.

igure 9. Relation between driving forces and absolute motion for the South American plate. ircles: Poles of absolute-motion vectors for the South American plate, according to models AM1- (Minster & Jordan 1978), Gordon & Jurdy (1986, labelled G&J), Chase (1978), HS2-NUVEL1 Gripp & Gordon 1990; see also DeMets *et al.* 1990). Triangle: pole of integrated torque vector of riving force (ridge push).